JPET Fast Forward. Published on September 5, 2008 as DOI: 10.1124/jpet.108.139006
This article has not been copyedited and formatted. The final version may differ from this version.

Title Page:

Pamapimod, A Novel p38 MAP Kinase Inhibitor: Preclinical Analysis of Efficacy and Selectivity

Ronald J. Hill, Karim Dabbagh, Deborah Phippard, Ching Li, Rebecca T. Suttmann, Mary Welch, Eva Papp, Kyung W. Song, Kung-ching Chang, David Leaffer, Yong-Nam Kim, Richard T. Roberts, Tanja S. Zabka, Dee Aud, Joseph Dal Porto, Anthony M. Manning, Stanford L. Peng, David M. Goldstein and Brian R. Wong

Departments of Cellular and Molecular Pharmacology (R.J.H., D.P., R.S., M.W. K.S., K.C., D.A., A.M.M., S.L.P., B.R.W.), Biochemical Pharmacology (E.P.), In Vivo Pharmacology (K.D., D.L.,Y-N.K, R.T.R., J.D., Pathology (T.S.Z.), and Medicinal Chemistry (D.M.G.), Roche Pharmaceuticals, Palo Alto, CA; Kennedy Institute of Rheumatology (C.L.), Imperial College, London, UK; Immunology Research (A.A.M), Biogen Idec, Cambridge, MA.

Running Title Page:

Running Title: Preclinical evaluation of the novel p38 inhibitor pamapimod

Corresponding author:

Ronald J. Hill, Ph.D.
Inflammation Discovery
Roche Pharmaceuticals
3431 Hillview Ave.
Palo Alto, CA 94304

Tel: 650-354-7804
Fax: 650-855-5501

Email: ronald.hill@roche.com

Text pages: 27 with refs
Tables: 4
Figures: 6 plus two supplemental
References: 40
Abstract: 247 words
Introduction: 748 words
Discussion: 1263 words

Abbreviations:

RA, rheumatoid arthritis ; JNK, c-Jun N terminal kinase ; RSK, ribosomal S6 kinase; NLK, Nemo-like kinase ; HSP, heat shock protein ; LPS, lipopolysaccharide ; TNF, tumor necrosis factor ; MAPK, mitogen-activated protein kinase ; TLR, toll-like receptor ; IL-1/6, interleukin-1/6 ; FBS, fetal bovine serum ; DMSO, dimethylsulfoxide ; SDS, sodium dodecylsulfate ; EDTA, ethylenediaminetetraacetic acid ; EGTA, ethyleneglycoltetraacetic acid ; TBST, Tris-buffered saline with tween-20 ; CDK, cyclin-dependent kinase; GSK3, glycogen synthetase kinase-3; CLK, Cdk2-like kinase; CMGC, Cdk, MAPK, GSK3, CLK kinase family; CT,

computerized tomography; EC50, efficacious concentration producing 50% inhibition; ED50, efficacious dose producing 50% inhibition; CI, confidence interval; HWB, human whole blood.

Recommended Section Assignment: Inflammation, Immunopharmacology and Asthma

Abstract

P38α is a protein kinase that regulates the expression of inflammatory cytokines, suggesting a role in the pathogenesis of diseases such as rheumatoid arthritis (RA) or systemic lupus erythematosis (SLE). Here we describe the pre-clinical pharmacology of pamapimod, a novel p38 MAP kinase inhibitor. Pamapimod inhibited p38α and p38β enzymatic activity with IC50s of 0.014 uM ± 0.002 uM and 0.48 uM ± 0.04 uM, respectively. There was no activity against p38δ or p38γ isoforms. When profiled across 350 kinases, pamapimod bound only to four kinases in addition to p38. Cellular potency was assessed using phosphorylation of HSP-27 and c-Jun as selective readouts for p38 and JNK, respectively. Pamapimod inhibited p38 (IC50 of 0.06 uM), but inhibition of JNK was not detected. Pamapimod also inhibited LPS-stimulated TNFα production by monocytes, IL-1β production in human whole blood, and spontaneous TNFα production by synovial explants from RA patients. LPS- and TNFα-stimulated production of TNFα and IL-6 in rodents also was inhibited by pamapimod. In murine collagen-induced arthritis (mCIA), pamapimod reduced clinical signs of inflammation and bone loss at 50 mg/kg or greater. In a rat model of hyperalgesia, pamapimod increased tolerance to pressure in a dose-dependent manner suggesting an important role of p38 in pain associated with inflammation. Finally, an analogue of pamapimod that has equivalent potency and selectivity inhibited renal disease in lupus-prone MRL/lpr mice. Our study demonstrates that pamapimod is a potent, selective inhibitor of p38α with the ability to inhibit the signs and symptoms of RA and other autoimmune diseases.

Introduction

Diseases of chronic inflammation such as rheumatoid arthritis (RA), psoriatic arthritis, and inflammatory bowel disease are driven by the release of pro-inflammatory cytokines and other mediators that disrupt normal tissue integrity. The synthesis and release of these mediators are controlled by various signaling pathways that are integrated largely by the mitogen-activated protein kinases (MAPKs). One of these MAPKs, p38, has been implicated in the regulation of a variety of immune cell functions (Schieven, 2005). A range of stimuli can activate p38 including toll-like receptor (TLR) ligands, TNF-alpha, IL-1 and cellular stresses such as heat shock and hypoxia (Chen et al., 2001; Karin, 2005). Upon activation, p38 regulates a range of genes that are implicated in the inflammatory response such as TNF-α, IL-1, IL-6 and many others (Zhang et al., 2007).

The role of p38 in response to and regulation of inflammatory pathways has led to efforts to develop inhibitors of p38 as therapeutic agents for diseases characterized by chronic inflammation (Kumar et al., 2003; Goldstein and Gabriel, 2005; Westra and Limburg, 2006). Involvement of p38 in the pathogenesis of RA is indicated by its activation in the synovial tissue of RA patients (Schett et al., 1998; Inoue et al., 2006). The potential of p38 inhibitors to inhibit human disease progression is suggested by their efficacy in rodent models of arthritis (Badger et al., 1996; Nishikawa et al., 2003; Wada et al., 2005; Medicherla et al., 2006). In addition, based on the role of p38 in secretion of TNF and the success of anti-TNF therapies in RA, several p38 inhibitors have been tested in clinical trials as a therapy for RA. Unfortunately, poor safety profiles have been observed in phase II clinical trials, due to adverse effects on the central nervous system and liver (Zhang et al., 2007). To date the presence of these dose-limiting

toxicities have prevented adequate exploration of efficacy which underscores the importance of separating p38-driven effects from the potentially toxic off-target effects of these compounds.

The specific effects of p38 inhibition have been investigated using both murine knock out models and pharmacologic inhibitors of p38. There are four isoforms of p38 (α, β, δ, γ) that demonstrate differential tissue expression (Hale et al., 1999; Alonso et al., 2000; Court et al., 2002) and activation (Alonso et al., 2000). The commonly used (but not selective) p38 inhibitors, SB203580 and SB202190, have equivalent potency against both the α and β isoforms, but do not inhibit the δ and γ isoforms (Kumar et al., 2003; Saklatvala, 2004). These compounds are effective inhibitors of inflammation indicating the importance of p38 α and/or β in inflammatory responses. Mice deficient in p38β, however, are viable and healthy and showed normal downstream signaling, immediate early gene transcription, LPS-induced cytokine production, as well as T cell development. In addition these mice remained susceptible to inflammatory disease when crossed onto the TNFα overexpressing TNFΔARE mouse line (Beardmore et al., 2005). In contrast, mice deficient in p38α are embryonic lethal due to a placental defect (Adams et al., 2000; Allen et al., 2000; Mudgett et al., 2000). Taken together, these data are consistent with the α isoform being the major contributor to the role of p38 in inflammation.

In addition to the effects of p38 inhibitors on various p38 isoforms, selectivity against other protein kinases is an important consideration in understanding the biology of p38 inhibition. As most kinase inhibitors in development target the binding site for the common substrate ATP, designing a selective ligand requires the identification of unique interaction sites around the ATP binding pocket. Discerning the degree of selectivity depends on the number of

different kinases that can be screened with a compound. In addition, despite with the availability of technologies that allow screening of large numbers of kinases (Fabian et al., 2005), these technologies do not allow a comparable level of selectivity assessment in cells in which cellular context can change the efficacy of inhibitors dramatically. This limitation has important implications for our understanding of p38 biology because the compounds that have been used widely to test the effects of p38 inhibition on various cell types are not completely selective in vitro (Fabian et al., 2005), and furthermore their selectivity in cells has not been characterized.

In the current study we present evidence that the p38 inhibitor pamapimod, currently in clinical development, is highly selective both in vitro and in cell culture. Additionally, the preclinical data support the conclusion that pamapimod has the ability to inhibit the signs and symptoms of RA as well as other autoimmune disease.

Methods

Kinase isoform selectivity assays. Purified recombinant human active p38α, β, γ or δ [10nM] diluted in 20mM MOPS, pH 7.2, 25mM betaglycerophosphate, 5mM EGTA, 1mM DTT, 1mM Na orthovanadate, 40mM MgCl2 was mixed with 10x pamapimod at a final concentration of [100 μM-0.0003 μM] in a 96-well plate (Greiner Bio), and incubated for 10 minutes at room temperature. The kinase reaction was initiated by the addition of 10 μl 4x substrate cocktail containing Km concentrations of the substrate recombinant myelin basic protein (Invitrogen) [30 μM], ATP (Roche Biosciences, Indianapolis, IN) [40 μM], and ^{33}P γATP (Amersham Inc, Piscataway, NJ) [2 μCi/rxn]. After a 30 minute incubation at 30°C, the reaction was terminated by the transfer of 25 μl of the reaction mixture to a phosphocellulose membrane/plate (Millipore Inc., Billerica, MA), containing 150 μl 0.75% phosphoric acid (Mallinckrodt Phillipsburg, NJ). The following day the free nucleotides in the membrane were washed under vacuum with 3x200 μl 0.75% phosphoric acid. After the last wash, membrane/plates are transferred to an adaptor plate (Packard), and 70 μl scintillation cocktail (Packard) was added to each well. After at least 4 hours, signal development the amount of radioactivity was counted on a top counter.

Inhibition of TNF-α secretion by a human monocytic cell line, THP-1. THP-1 cells, growing in log phase, were collected by centrifugation and resuspended in RPMI (Gibco BRL, #11875-085) containing 5.5 X 10^{-5} M 2-mercaptooethanol (Gibco, #21985-023), and 10% fetal bovine serum (FBS) (Summit, #FS-110-05) to a final cell concentration of 2.5 x 10^{6} cells per ml. Dilutions of pamapimod were pre-dispensed in 25 uL aliquots (before addition of cells) into round-bottom 96-well plates (U bottom TC plate; Costar #3799). The starting concentration was

100 uM in 5% DMSO and 6 half log serial dilutions were made. After the addition of 200 uL cell suspension and 25 uL of 5 ug/ml lipopolysaccharide (LPS, E. coli; 0127; B8; Cat. No. L3129, Sigma Chem Co, St. Louis, MO) in medium, the final DMSO concentration was 0.5%. Compounds were diluted an additional 10-fold and the final LPS concentration was 500 ng/mL. The cell suspensions and compound dilutions were combined and incubated for 30 minutes at 37°C in a 5% CO2 humidified atmosphere, prior to addition of LPS (or medium for non-LPS control samples). Following addition of LPS, plates were incubated for 2 hours followed by centrifugation to pellet cells. Cell supernatants were stored at 4°C until analyzed for TNF-α content. TNF-α levels were determined by Elisa (Antibody Solutions, Palo Alto, CA) following the manufacture's directions. Cytokine concentrations were determined from a standard curve using Molecular Devices SoftMax Pro. The percent inhibition was calculated for each pamapimod concentration tested and an IC50 curve was constructed using Xlfit software.

Inhibition of IL-1β biosynthesis in LPS-stimulated human whole blood. Blood was collected from healthy volunteers (drug-free for two weeks) into vacutainers (Becton Dickinson, Mountainview, CA) containing 19 units/ml sodium heparin. Pamapimod was pre-dispensed and diluted as described for the THP-1 assay above. Human whole blood (200 uL per sample) was pre-incubated with the diluted compound for 30 minutes at 37°C followed by addition of 25 uL of LPS dissolved in RPMI (Gibco BRL, #11875-085) to produce a final LPS concentration of 0.5 ug/ml. Negative control wells received RPMI alone. Plates were incubated for 18 hours at 37°C in a 5% CO_2 atmosphere followed by centrifugation at 150 x g for 10 minutes. Plasma was collected from each sample and stored in polypropylene plates at 4°C. For IL-1β determinations, plasma was diluted 4-fold in ELISA wash buffer and tested by ELISA (Antibody Solutions, Palo

Alto CA) following the manufacturer's instructions. Cytokine levels were detected and calculated as described above for the THP-1 assay.

Detection of p38 and JNK activity in cells or tissue samples by Western blotting. Selectivity of inhibition of p38 and JNK in a cellular context was determined by measuring phosphorylation of HSP-27 and c-Jun, respectively in SW-1353 or THP-1 cells. After 30 min pretreatment with pamapimod, cells were stimulated with TNFα (R&D, Minneapolis, MN) for 20min. and then rinsed with ice cold phosphate buffered saline and lysed in 100ul of ice cold lysis buffer (20 mM Tris pH7.5, 150 mM NaCl, 1mM, EDTA, 1mM, EGTA, 1% Triton X-100, 2.5 mM sodium pyrophosphate, 1mM beta-glycerolphosphate, 1mM Na_3V0_4 (Cell signaling Technologies, Danvers, MA) plus protease inhibitor mixture (Roche Applied Science, Indianapolis, IN). After sonicating ten times for 1 second each on ice, the samples were centrifuged at 12,000 x g for 5 min at 4^{o}C. The protein concentration was measured, and 15ug of protein from each sample was separated by SDS-polyacrylamide gel electrophoresis and transferred to nitrocellulose membranes. Membranes were blocked in TBST buffer (20mM Tris pH7.5, 136mM NaCl , 0.1% Tween 20) containing 5% milk and incubated with the primary antibodies for phospho-HSP27, phospho-cJun, phospho-p38, p38, HSP27 (1:1000 dilution in TBST containing 5% BSA: Cell Signaling Technologies), and c-Jun (1:1000 dilution in TBST containing 5% BSA: Chemicon, Temecula, CA). Western blots of cell lysates were analyzed by the addition of IR Dye 700 Dx goat anti-rabbit and IR Dye 800 goat anti-mouse antibodies (Rockland Immunochemicals, Philadelphia, PA) and the multicolor fluorescence detected with the Odyssey imaging system (Li-Cor Biosciences, Lincoln, NE). Density of phospho-protein bands was measured using ImageQuant software (Amersham, Inc.). The percent inhibition of pamapimod treated phospho-

protein, normalized with level of total protein, was calculated and an IC50 curve was constructed using Xlfit software.

To demonstrate modulation of p38 activity in vivo, phosphorylation of HSP-25 in tissues from either DBA/1J (mCIA model) or MRL/lpr (lupus model) mice was assessed by Western blotting after dosing with pamapimod. Tissue lysates from lung or inguinal lymph nodes were prepared by homogenization in 10 mM Tris, 100 mM NaCl, 1 mM EDTA, 1 mM EGTA, 1 mM sodium fluoride, 20 mM sodium phosphate, 2 mM sodium vanadate, 1% Triton X-100, 10% glycerol, 0.1% SDS and 0.5% deoxycholate (Biosource International #FNN0011) with protease inhibitors. Western blots were probed for total HSP-25 (Santa Cruz Biotechnology), phospho-HSP-25 (Biosource International), total p38 and phospho-p38 (Cell Signaling) and analyzed either by the addition of horseradish peroxidase coupled secondary antibodies and developed with the enhanced chemiluminescence (ECL) detection system (Amersham Inc., Piscataway, NJ) or by the addition of Alexa Fluor 647 goat anti-mouse (Molecular Probes Inc.) and the multicolor fluorescence detected with the Typhoon imaging system (Amersham, Inc.).

Murine acute LPS - induced cytokine production models. All animal procedures were approved by and conducted in accordance with the Roche Palo Alto Institutional Animal Care and Use Committee guidelines. Female BALB/c mice (Jackson Laboratories, Bar Harbor, MA) were utilized for *in vivo* LPS or TNF-α stimulation studies. In all experiments each dose group consisted of 8 animals (each 18-25 g in weight). The test materials were administered in a volume of 1 ml/100 g of body weight as suspensions in an aqueous vehicle containing 0.9% NaCl, 0.5% sodium carboxymethylcellulose, 0.4% polysorbate 80, 0.9% benzyl alcohol, and 97.3% distilled water. Mice were orally administered vehicle or the indicated doses of

pamapimod 30 minutes prior to LPS (E. coli, serotype 0127:b8; Sigma, St. Louis, MO) or TNF-α intraperitoneal challenge. LPS was administered to mice at 800μg/kg. Animals were euthanized via CO_2 inhalation 1.5 hours after LPS or TNF-α administration, and blood was collected and transferred to SST® vacutainer serum separator tubes. The sera were separated and stored at -20°C until analysis by ELISA. ELISA kits for TNF-α and IL-6 were obtained from Biosource International (Camarillo, CA). All ELISAs were performed according to manufacturer specifications.

Brewer's yeast-induced paw hyperalgesia model. In order to measure effects of p38 inhibition on inflammatory pain, we utilized the Randall-Selitto test of mechanical hyperalgesia. Male Sprague-Dawley rats (115-150g; Charles River Laboratories, Hollister, CA) were acclimated for one week and randomized into groups of 10 animals each. A solution of 20% brewers yeast (0.1 ml; Sigma) was injected into the left hind paw of each animal at the beginning of the study. Two hours later, rats were orally administered vehicle (1 ml/kg), indomethacin (5.0 mg/kg) or pamapimod at doses of 10 – 100 mg/kg. After 1 additional hour, the left hind paw of each rat was placed on the platform of the Basile Analgesy-meter and the mechanical force in grams at which the rat withdraws its paw is recorded. Following the assay, the animals were euthanized via CO2 asphyxiation and bled for serum collection.

Murine collagen – induced arthritis model. DBA/1J female mice (Jackson Laboratories, Bar Harbor, ME) were between 8-10 weeks of age at the initiation of the experiments. Each dose group consisted of 12 animals. Test materials were administered in a volume of 0.2 ml in the aqueous vehicle described above. On day 0 mice were injected intra-dermally at the base of the tail with 0.1 ml of an emulsion of Bovine Type II Collagen (100μg; Chondrex, LLC, Seattle,

WA) and an equal volume of Complete Freunds adjuvant (H37 RA; Difco Laboratories, Detroit, MI). Approximately 4 weeks after collagen injection the animals were challenged with an i.p. injection of LPS (50μg). Mice were scored daily after LPS challenge for the development of arthritis in paws until disease became evident (mean clinical score=3-4). Following detection of disease in the majority of animals the mice were randomized into dosing groups and treatment was initiated. Mice displaying no arthritis or disease outside worse than the target clinical score were removed from the studies. Pamapimod and vehicle were administered by oral gavage (0.2 ml) once daily. Scoring was as follows: 1= swelling and/or redness of paw or one digit. 2= swelling in two or more joints. 3= gross swelling of the paw with more than two joints involved. 4= severe arthritis of the entire paw and digits. The arthritic index for each mouse is determined by adding the four scores of the individual paws.

To measure effects on bone destruction, ex vivo micro-CT imaging and analysis was performed on the calcaneous, tarsal bones and phalanges of formaldehyde-fixed paw samples. Regions of interest were hand drawn over the reconstructed ct images of the calcaneous and tarsal bones. A 2.1 mm diameter region of interest was centered over the metatarsal-phalangeal joint of each toe. The bone volume was calculated from each of these regions of the paw. The bone volumes did not include the lower density periosteal bone formed in diseased tissue.

Histopathology of kidneys from MRL/MpJ-Fas^{lpr}/J (MRL/lpr) mice. MRL/MpJ-*Fas*^{lpr}/J (MRL/lpr), mice from the Jackson Laboratory (Stock # 006825) were maintained under specific pathogen-free conditions. Necropsy was performed on sacrificed mice, and one kidney from each animal was fixed in 10% neutral-buffered formalin. The kidney was cross-sectioned into four quadrants with the first sections made on either side of the renal papilla and the second sections

made lateral to the first. This method enabled review of each renal pole and the renal papilla with arcuate vessels. Sections were paraffin-embedded, sectioned at 5 μm thick, stained with hematoxylin and eosin, and reviewed by light microscopy. In a subset of animals, serial 3 μm thick sections were stained with periodic acid-Schiff stain for mucopolysaccharide-based material (including fibrin and glomerular deposition of non-collagenous material). The histopathology parameters evaluated were arteritis, glomerulonephritis, and perivascular mononuclear infiltration. Arteritis was recorded as the total number of vessels affected across the four sections to the exclusion of the juxtaglomerular apparatus. Glomerulonephritis was recorded as 1-5 according to the most severe morphologic pattern identified from one of the five morphologic patterns of lupus glomerulonephritis as defined by the World Health Organization (Appas, 2005). The perivascular mononuclear infiltrate was scored as 1-5 according to the average from all vessels across all four sections and based on the average width of the band between the vein and proximate arteriole, or in the papilla, as the average width of the band between the renal vein and urinary space and interlobular vein and artery (1= minimal or few leukocytes; 2 = mild or < 1x tubular diameter; 3 = moderate or ≤ 2 x tubular diameter; 4 = marked or > 2x – 4x tubular diameter; 5 = severe or > 4 x tubular diameter).

Cultured synovial explants from rheumatoid arthritis patients: Synovium from patients with rheumatoid arthritis undergoing joint surgery was dissociated by cutting into small pieces, followed by digestion with collagenase type IV and DNAse I (Sigma). The mixed cell suspension was cultured for 2 days in the presence or absence of pamapimod at 1-2 x 10^6 cells/ml in RPMI 1640 containing 5% heat inactivated FCS, 2 mM L-glutamine and antibiotics. Supernatants were removed and assayed by ELISA for TNFα.

Results

Kinase selectivity profiling of pamapimod:

We initially sought to characterize the selectivity of pamapimod, which is a typical ATP competitive kinase inhibitor that binds the hinge region and interacts with both the front and back pockets of the ATP binding site of p38. The selectivity of pamapimod against a panel of 350 kinases was assessed using the ATP binding site competition assay developed by Ambit Biosciences (San Diego, CA). This technology utilizes phage displayed kinases that are immobilized with non-selective inhibitors. Elution of these immobilized kinases with test compounds reflects the affinity of the compound for a given binding domain. As demonstrated in Figure 1, pamapimod was quite selective and other than p38, interacted mainly with JNK isoforms, which similarly to p38 are members of CMGC family (Manning et al., 2002) (Table 1). In addition, pamapimod interacted with one member of the casein kinase family, Nemo-like kinase (NLK) and two isoforms of the ribosomal S6 kinase, RSK. Table 2 shows the activity of pamapimod against the four p38 isoforms. Similar to previous p38 inhibitors that have been developed, pamapimod preferentially inhibits the alpha and beta isoforms without activity against the delta or gamma isoforms. Table 1 presents Kd values for the kinases from the Ambit screen that showed greater than 85% inhibition at 10 uM concentration. These data indicate that inhibition of the Jnk isoforms could occur in the same concentration ranges as p38 inhibition.

Since both p38 and JNK are implicated in inflammatory responses, it was necessary to determine whether the activity of pamapimod against p38 and JNK activities detected by phage display would be reflected in cellular activity as well. To assess this, multiplexed substrate phosphorylation assays were performed. Human bone chondrosarcoma cells (SW-1353) were

stimulated with TNF and phospho-c-Jun and phospho-Hsp27 were quantified by western blots as a reflection of cellular JNK and p38 activity, respectively (Figure 2). Despite the relatively high affinity of JNK for pamapimod in Ambit profiling, pamapimod was not potent (IC50 >10uM) in cells as an inhibitor of JNK. Similar results were obtained using TNFα stimulation of the monocytic cell line THP-1 (Suppl Fig 1). These findings underscore the importance of using cell-based assays to confirm selectivity demonstrated by cell-free binding methods. In addition, it established that the anti-inflammatory activities of pamapimod are likely to occur through a p38 mechanism.

Anti-inflammatory activities of Pamapimod:

Next, the effects of pamapimod on cytokine production were studied *in vitro* and *in vivo*. We focused on the production of TNFα, Il-1β and IL-6 since these cytokines are known to be regulated by p38 and are critical in autoimmune disease. The *in vitro* results are summarized in Table 3. Following LPS-stimulation of the human myelomonocytic cell line (THP-1), secretion of TNFα was inhibited by pamapimod with an EC50 of 0.025 ± 0.01 uM. In order to incorporate the potential effects of serum binding on the efficacy of pamapimod, we also stimulated human whole blood with LPS and again monitored cytokine production. Pamapimod suppressed TNFα and IL-1β production in whole blood with EC50s of 0.40 ± 0.16 uM and 0.10 ± 0.03 uM, respectively. This represents an approximately 16-fold shift in efficacy when 100% human serum was present compared with 10% fetal bovine serum used for the THP-1 cell assays.

We then studied the effects of pamapimod on acute inflammation in vivo by evaluating LPS-and TNFα–stimulated cytokine production in rodents and in a rat model of hyperalgesia

JPET Fast Forward. Published on September 5, 2008 as DOI: 10.1124/jpet.108.139006
This article has not been copyedited and formatted. The final version may differ from this version.

(Table 4). ED50s required to suppress TNFα and IL-6 were achieved at plasma levels in the same range as observed for efficacy in human whole blood. In the rat model of hyperalgesia, pamapimod, tested at 10 – 100 mg/kg, increased tolerance to pressure-induced pain responses in a dose-dependent manner (effective dose associated with half-maximal effect [ED_{50}] = 20 mg/kg), suggesting that pamapimod may reduce the pain associated with inflammation. A previous study also demonstrated reversal of inflammatory mechanical hyperalgesia induced by injection of complete Freund's adjuvant into the hindpaw (Ganju et al., 2001). Note the higher ED50 observed for the hyperalgesia model compared with the acute cytokine release is likely due to the necessity to overcome pre-established inflammation in the model and the requirement to penetrate joint tissue.

The ability of pamapimod to suppress chronic inflammation was studied using a mouse model of RA. Figure 3 demonstrates that pamapimod suppressed clinical scores for collagen-induced arthritis in a dose-dependent manner, achieving significance at 100 mg/kg or greater. For doses of 50 mg/kg or greater, the 24 hour plasma concentration of pamapimod was maintained above the EC50 values for the acute in vivo inflammation models (Table 4) as well as the IC50 values for HWB LPS-induced cytokine production (Table 2). Modulation of p38 activity in vivo was confirmed by measurement of HSP-25 phosphorylation in inguinal lymph nodes at the end of the study (data not shown). Dosing was oral, once per day, initiated 4 days after the onset of symptoms. Thus pamapimod was effective when administered in a therapeutic manner (as opposed to a prophylactic dosing schedule).

Bone protection by pamapimod in murine collagen-induced arthritis

Micro-CT analysis was used to measure bone volume in mice treated with increasing doses of pamapimod in the murine collagen-induced arthritis model described above. In the combined phalanges scores, both the 90mg/kg and the 150mg/kg groups had significantly higher bone volumes than the controls (Figure 4a). Decreased bone damage with pamapimod can be visualized in the micro CT images shown in Figure 4b, which compares naive, vehicle control and the 150 mg/kg dose. The measured bone volumes did not include the lower density periosteal bone formed in diseased tissue. Histology was performed on paws from the same animals that received pamapimod for the micro-CT study (Figure 4c). Scoring was performed for the following parameters: cartilage degeneration, periosteal new bone formation, bone erosion, soft tissue proliferation and inflammation, and pannus and joint space exudates. All parameters except joint space exudates, including the total scores, were significantly decreased at the 90 and 150 mg/kg doses, consistent with the findings in the micro-CT study. Joint space exudate was decreased but did not reach significance.

Pamapimod suppresses spontaneous production of TNFα by synovial explants from RA patients:

In order to evaluate the potential effects of pamapimod on inflammation in diseased joints of human RA, spontaneous production of TNFα from synovial explants was measured following treatment with pamapimod for 2 days at varying concentrations. As shown in figure 5A, pamapimod inhibited TNFα production by the synovial explants with an IC50 (95% CI) of 0.104 uM (0.048 – 0.23 uM), which is similar efficacy to that observed for inhibition of LPS-induced cytokine production in human whole blood. Thus, assuming the tissue levels of pamapimod are similar to those achieved in the plasma, the inhibition of cytokine production in

whole blood could be a surrogate for inhibition of inflammatory cytokines in the diseased joint and could be used as a pharmacodynamic assay to predict efficacious dosing. Additionally, on comparing the efficacy of pamapimod with that of SB203580 (Figure 5B), which is the widely used reference compound for p38 inhibition, SB203580 had a similar IC50 (95% CI) of 0.240 uM (0.015 – 3.7 uM) in the explant model. In performing this study we observed that there was a subset of patients who were partial responders, i.e. they did not achieve full inhibition with drug. This partial response occurred at a rate of approximately one in three donors.

Efficacy of p38 inhibition in a spontaneous mouse model of lupus:

To assess the role of p38 in lupus, spontaneous lupus-prone MRL/lpr mice were treated with R9111, an analogue of pamapimod with equivalent kinase selectivity (see Suppl Fig 2) and potency against LPS-induced cytokine production (TNFα from THP-1 cells EC50 = 0.03 ± 0.02 uM; IL-1β from whole blood EC50 = 0.07 ± 0.04 uM). R9111 was administered by mini-pump beginning at 12-14 weeks of age for 2 weeks (Fig 6). Whereas vehicle-treated animals exhibited renal disease as evidenced by significant proteinuria and histopathological evidence of lupus glomerulonephritis, perivascular leukocyte infiltration, and occasionally arteritis, treatment with R9111 significantly reduced both proteinuria and total perivasculitis scores (Figs 6a and 6b), the former comparable if not superior to dexamethasone treatment. These findings correlated with the ability of R9111 to inhibit p38 activity *in vivo*, as evidenced by blockade of phosphorylation of the p38 substrate Hsp25 (Fig 6c). Thus, in a short-term administration regimen, the analogue of pamapimod, R9111, was effective in the treatment of MRL/lpr renal disease.

Discussion

The current study characterized the *in vitro* and *in vivo* potency of the small molecule inhibitor of p38 MAP kinase, pamapimod. A binding assay to profile pamapimod against 350 other protein kinases, demonstrated that the molecule is highly selective, binding only to JNK, another MAPK family member, with affinity comparable to p38. However, despite the apparent affinity for JNK, evaluation of Jnk inhibition in two cell types based on phosphorylation of c-Jun, demonstrates that in cells pamapimod is not potent against JNK. Thus, in vivo pamapimod is anticipated to have little or no direct impact on Jnk activity.

The isoform selectivity of pamapimod is similar to that observed for other small molecule inhibitors of p38, as it only inhibits only the α and β isoforms but not the γ and δ isoforms (Kumar et al., 2003; Saklatvala, 2004). This selectivity is consistent with sequence analysis that indicates the α and β isoforms form a subgroup distinct from that of γ and δ with only 60% homology between the subgroups (Cohen, 1997). The β isoform is minimally expressed in inflammatory cells and preferentially expressed in endothelial cells (Hale et al., 1999). Data from this study indicate that pamapimod is selective for the α isoform by 34-fold or 92-fold based on enzyme IC50 or binding Kd, respectively. The δ isoform is expressed by monocytes, macrophages, lymphocytes and neutrophils (Hale et al., 1999) but is not targeted by pamapimod and therefore is not part of the mechanism of action. Accordingly, these findings suggest that pamapimod inhibits inflammation through its activity against p38α.

The finding that p38 was a target of the pyridinyl imidazoles that block LPS-induced TNF-α and IL-1β release from monocytes (Lee et al., 1994) initiated over a decade of work to

define the role of p38 in inflammatory processes. p38 is ideally positioned to integrate signaling from cytokines and growth factors and to convert these signals into transcription of inflammatory cytokines, matrixmetalloproteinases and Cox-2 and other effectors; therefore it has become an attractive target for therapeutic inhibition of RA and other autoimmune diseases (reviewed in (Kumar et al., 2003; Goldstein and Gabriel, 2005; Schieven, 2005; Westra and Limburg, 2006)). p38 regulates cellular responses at multiple levels including transcriptional activation (Han et al., 1997; Wesselborg et al., 1997; Zhu and Lobie, 2000), post-transcriptional mRNA stability (Winzen et al., 1999; Frevel et al., 2003; Dean et al., 2004), translation (Brook et al., 2000) and phosphorylation of downstream kinases such as MAPKAPK-2 (Brook et al., 2000). In addition, p38 appears to regulate cytokine and chemokine gene expression by recruitment of NK-κB to cryptic binding sites through a mechanism involving phosphorylation of histone H3 (Saccani et al., 2002). The current study demonstrates that pamapimod inhibits LPS-induced release of TNFα and IL-1β both in vitro and in vivo, which is consistent with the reported role for p38 in regulation of inflammatory cytokines. It also demonstrates that pamapimod inhibits phosphorylation of HSP-27, a substrate of MAPKAPK-2, which indicates p38 signals through MAPKAPK-2.

The effects of pamapimod on collagen-induced arthritis in mice are consistent with previous studies of p38 inhibitors (Badger et al., 1996; Nishikawa et al., 2003; Wada et al., 2005; Medicherla et al., 2006). However, the current study is the first to characterize an exquisitely selective p38 inhibitor thus strongly suggesting that the observed disease modification occurs solely through a p38 mechanism. This finding is important because collagen-induced arthritis in mice can be inhibited by a variety of immune modulators. Also, previous compounds shown to

have efficacy in the rodent models of arthritis had significant off-target activity which could have contributed to the disease modification as well as adverse side effects (Fabian et al., 2005; Goldstein and Gabriel, 2005; Zhang et al., 2007). However, it is noteworthy that in a recent Phase II trial of pamapimod, elevation of liver transamidase levels and Cmax-related dizziness in some patients was reported (Cohen et al.). Therefore p38 target selectivity does not eliminate all liver and CNS side effects.

The inhibition of bone loss as demonstrated in this study, also has been reported previously with p38 inhibitors (Badger et al., 1996; Nishikawa et al., 2003; Medicherla et al., 2006). In one other study that reported decreased bone loss with a p38 inhibitor there was a concomitant decrease in osteoclasts (Medicherla et al., 2006), presumably due to the role of p38 in osteoclast differentiation (Li et al., 2002; Pargellis and Regan, 2003). This outcome is potentially beneficial in treatment of RA with p38 inhibitors because current therapies have poor efficacy against cartilage and bone loss. In addition, the effect of pamapimod on inflammatory pain is another potential benefit in a therapeutic setting. A previous study with a p38 inhibitor, SB203580, also demonstrated reversal of inflammatory mechanical hyperalgesia induced by injection of complete Freund's adjuvant into the hindpaw (Ganju et al., 2001). In addition, there are many studies showing that p38 inhibitors can attenuate inflammatory pain (reviewed in (Ji et al., 2007)).

The elevation of cytokines in rheumatoid synovium is clearly a key component to the ongoing chronic inflammation of RA. Thus the finding that p38 inhibition suppresses the spontaneous production of TNFα in synovial explants is encouraging because it suggests that pamapimod may inhibit cytokine release in the joints of RA patients. A previous study with the

p38 inhibitor SB203580 reported low potency against TNFα produced by rheumatoid synovial explants compared to primary macrophages (Campbell et al., 2004). In this study, however, both pamapimod and SB203580 were effective against TNFα produced by diseased synovial explants as LPS-induced TNFα from other primary human cells. The reason for this discrepancy with previous work is not clear. Our observation that 1/3 of donors only responded partially to inhibition by pamapimod may have significance in predicting clinical response rates.

The involvement of p38 in the response to and production of multiple inflammatory cytokines suggests that inhibition of this target should have utility in other autoimmune diseases in addition to RA. This study demonstrated activity of a pamapimod analog against the spontaneous development of nephritis in MRL/lpr mice suggesting that p38 inhibition may be an efficacious treatment for lupus as well. A previous study using the same murine animal model implicated p38 in the progression of Lupus-like disease by demonstrating elevation of p38 phosphorylation (Iwata et al., 2003). The study also used FR167653, a p38 inhibitor, to reduce kidney pathology which correlated with a reduction in p38 phosphorylation. Although the compound is reported to be selective, its effects were presumably upstream in the pathway because p38 phosphorylation is not dependent on p38, but rather on the activity of MKK3 and MKK6. The current study demonstrated that direct inhibition of p38 activity as confirmed by a decrease in phosphorylation of a p38-dependent substrate, HSP-25, correlated with reduced proteinuria and histopathology, namely the findings of mononuclear perivasculitis. These data combined with our selectivity profiling for pamapimod demonstrate that the amelioration of pathology is dependent on inhibition of p38 activity.

In summary, the current study demonstrates pamapimod to be a highly selective inhibitor of p38 when profiled across 350 kinases by competitive binding assays and also when profiled in cells by phosphorylation of selective substrates. This selectivity may translate into a better safety and tolerability profile which could allow full exploration of its pharmacology in humans. The anti-inflammatory activities of pamapimod in cells and *in vivo* indicate the potential to alleviate the signs and symptoms of RA as well as to provide bone protection. In addition, the efficacy of a pamapimod analog in an animal model of renal lupus suggests the potential utility of p38 inhibition for autoimmune diseases other that RA.

References

Adams RH, Porras A, Alonso G, Jones M, Vintersten K, Panelli S, Valladares A, Perez L, Klein R and Nebreda AR (2000) Essential role of p38alpha MAP kinase in placental but not embryonic cardiovascular development. *Mol Cell* **6**:109-116.

Allen M, Svensson L, Roach M, Hambor J, McNeish J and Gabel CA (2000) Deficiency of the stress kinase p38alpha results in embryonic lethality: characterization of the kinase dependence of stress responses of enzyme-deficient embryonic stem cells. *J Exp Med* **191**:859-870.

Alonso G, Ambrosino C, Jones M and Nebreda AR (2000) Differential activation of p38 mitogen-activated protein kinase isoforms depending on signal strength. *J Biol Chem* **275**:40641-40648.

Badger AM, Bradbeer JN, Votta B, Lee JC, Adams JL and Griswold DE (1996) Pharmacological profile of SB 203580, a selective inhibitor of cytokine suppressive binding protein/p38 kinase, in animal models of arthritis, bone resorption, endotoxin shock and immune function. *J Pharmacol Exp Ther* **279**:1453-1461.

Beardmore VA, Hinton HJ, Eftychi C, Apostolaki M, Armaka M, Darragh J, McIlrath J, Carr JM, Armit LJ, Clacher C, Malone L, Kollias G and Arthur JS (2005) Generation and characterization of p38beta (MAPK11) gene-targeted mice. *Mol Cell Biol* **25**:10454-10464.

Brook M, Sully G, Clark AR and Saklatvala J (2000) Regulation of tumour necrosis factor alpha mRNA stability by the mitogen-activated protein kinase p38 signalling cascade. *FEBS Lett* **483**:57-61.

Campbell J, Ciesielski CJ, Hunt AE, Horwood NJ, Beech JT, Hayes LA, Denys A, Feldmann M, Brennan FM and Foxwell BM (2004) A novel mechanism for TNF-alpha regulation by p38 MAPK: involvement of NF-kappa B with implications for therapy in rheumatoid arthritis. *J Immunol* **173**:6928-6937.

Chen Z, Gibson TB, Robinson F, Silvestro L, Pearson G, Xu B, Wright A, Vanderbilt C and Cobb MH (2001) MAP kinases. *Chem Rev* **101**:2449-2476.

Cohen P (1997) The search for physiological substrates of MAP and SAP kinases in mammalian cells. *Trends Cell Biol* **7**:353-361.

Cohen SB, Cheng T, Chindalore V, Damjanov N, Burgos-Vargas R, DeLora P, Zimany K, Travers H and Caulfield JP Evaluation of the Efficacy and Safety of Pamapimod, a p38 MAP Kinase Inhibitor, in a Double-blind, Methotrexate-controlled Study in Patients with Active Rheumatoid Arthritis. *Arthritis Rheum* **In press**.

Court NW, dos Remedios CG, Cordell J and Bogoyevitch MA (2002) Cardiac expression and subcellular localization of the p38 mitogen-activated protein kinase member, stress-activated protein kinase-3 (SAPK3). *J Mol Cell Cardiol* **34**:413-426.

Dean JL, Sully G, Clark AR and Saklatvala J (2004) The involvement of AU-rich element-binding proteins in p38 mitogen-activated protein kinase pathway-mediated mRNA stabilisation. *Cell Signal* **16**:1113-1121.

Fabian MA, Biggs WH, 3rd, Treiber DK, Atteridge CE, Azimioara MD, Benedetti MG, Carter TA, Ciceri P, Edeen PT, Floyd M, Ford JM, Galvin M, Gerlach JL, Grotzfeld RM, Herrgard S, Insko DE, Insko MA, Lai AG, Lelias JM, Mehta SA, Milanov ZV, Velasco

AM, Wodicka LM, Patel HK, Zarrinkar PP and Lockhart DJ (2005) A small molecule-kinase interaction map for clinical kinase inhibitors. *Nat Biotechnol* **23**:329-336.

Frevel MA, Bakheet T, Silva AM, Hissong JG, Khabar KS and Williams BR (2003) p38 Mitogen-activated protein kinase-dependent and -independent signaling of mRNA stability of AU-rich element-containing transcripts. *Mol Cell Biol* **23**:425-436.

Ganju P, Davis A, Patel S, Nunez X and Fox A (2001) p38 stress-activated protein kinase inhibitor reverses bradykinin B(1) receptor-mediated component of inflammatory hyperalgesia. *Eur J Pharmacol* **421**:191-199.

Goldstein DM and Gabriel T (2005) Pathway to the clinic: inhibition of P38 MAP kinase. A review of ten chemotypes selected for development. *Curr Top Med Chem* **5**:1017-1029.

Hale KK, Trollinger D, Rihanek M and Manthey CL (1999) Differential expression and activation of p38 mitogen-activated protein kinase alpha, beta, gamma, and delta in inflammatory cell lineages. *J Immunol* **162**:4246-4252.

Han J, Jiang Y, Li Z, Kravchenko VV and Ulevitch RJ (1997) Activation of the transcription factor MEF2C by the MAP kinase p38 in inflammation. *Nature* **386**:296-299.

Inoue T, Boyle DL, Corr M, Hammaker D, Davis RJ, Flavell RA and Firestein GS (2006) Mitogen-activated protein kinase kinase 3 is a pivotal pathway regulating p38 activation in inflammatory arthritis. *Proc Natl Acad Sci U S A* **103**:5484-5489.

Iwata Y, Wada T, Furuichi K, Sakai N, Matsushima K, Yokoyama H and Kobayashi K (2003) p38 Mitogen-activated protein kinase contributes to autoimmune renal injury in MRL-Fas lpr mice. *J Am Soc Nephrol* **14**:57-67.

Ji RR, Kawasaki Y, Zhuang ZY, Wen YR and Zhang YQ (2007) Protein kinases as potential targets for the treatment of pathological pain. *Handb Exp Pharmacol*:359-389.

Karin M (2005) Inflammation-activated protein kinases as targets for drug development. *Proc Am Thorac Soc* **2**:386-390; discussion 394-385.

Kumar S, Boehm J and Lee JC (2003) p38 MAP kinases: key signalling molecules as therapeutic targets for inflammatory diseases. *Nat Rev Drug Discov* **2**:717-726.

Lee JC, Laydon JT, McDonnell PC, Gallagher TF, Kumar S, Green D, McNulty D, Blumenthal MJ, Heys JR, Landvatter SW and et al. (1994) A protein kinase involved in the regulation of inflammatory cytokine biosynthesis. *Nature* **372**:739-746.

Li X, Udagawa N, Itoh K, Suda K, Murase Y, Nishihara T, Suda T and Takahashi N (2002) p38 MAPK-mediated signals are required for inducing osteoclast differentiation but not for osteoclast function. *Endocrinology* **143**:3105-3113.

Manning G, Whyte DB, Martinez R, Hunter T and Sudarsanam S (2002) The protein kinase complement of the human genome. *Science* **298**:1912-1934.

Medicherla S, Ma JY, Mangadu R, Jiang Y, Zhao JJ, Almirez R, Kerr I, Stebbins EG, O'Young G, Kapoun AM, Luedtke G, Chakravarty S, Dugar S, Genant HK and Protter AA (2006) A selective p38 alpha mitogen-activated protein kinase inhibitor reverses cartilage and bone destruction in mice with collagen-induced arthritis. *J Pharmacol Exp Ther* **318**:132-141.

Mudgett JS, Ding J, Guh-Siesel L, Chartrain NA, Yang L, Gopal S and Shen MM (2000) Essential role for p38alpha mitogen-activated protein kinase in placental angiogenesis. *Proc Natl Acad Sci U S A* **97**:10454-10459.

Nishikawa M, Myoui A, Tomita T, Takahi K, Nampei A and Yoshikawa H (2003) Prevention of the onset and progression of collagen-induced arthritis in rats by the potent p38 mitogen-activated protein kinase inhibitor FR167653. *Arthritis Rheum* **48**:2670-2681.

Pargellis C and Regan J (2003) Inhibitors of p38 mitogen-activated protein kinase for the treatment of rheumatoid arthritis. *Curr Opin Investig Drugs* **4**:566-571.

Saccani S, Pantano S and Natoli G (2002) p38-Dependent marking of inflammatory genes for increased NF-kappa B recruitment. *Nat Immunol* **3**:69-75.

Saklatvala J (2004) The p38 MAP kinase pathway as a therapeutic target in inflammatory disease. *Curr Opin Pharmacol* **4**:372-377.

Schett G, Redlich K, Xu Q, Bizan P, Groger M, Tohidast-Akrad M, Kiener H, Smolen J and Steiner G (1998) Enhanced expression of heat shock protein 70 (hsp70) and heat shock factor 1 (HSF1) activation in rheumatoid arthritis synovial tissue. Differential regulation of hsp70 expression and hsf1 activation in synovial fibroblasts by proinflammatory cytokines, shear stress, and antiinflammatory drugs. *J Clin Invest* **102**:302-311.

Schieven GL (2005) The biology of p38 kinase: a central role in inflammation. *Curr Top Med Chem* **5**:921-928.

Wada Y, Nakajima-Yamada T, Yamada K, Tsuchida J, Yasumoto T, Shimozato T, Aoki K, Kimura T and Ushiyama S (2005) R-130823, a novel inhibitor of p38 MAPK, ameliorates hyperalgesia and swelling in arthritis models. *Eur J Pharmacol* **506**:285-295.

Wesselborg S, Bauer MK, Vogt M, Schmitz ML and Schulze-Osthoff K (1997) Activation of transcription factor NF-kappaB and p38 mitogen-activated protein kinase is mediated by distinct and separate stress effector pathways. *J Biol Chem* **272**:12422-12429.

Westra J and Limburg PC (2006) p38 mitogen-activated protein kinase (MAPK) in rheumatoid arthritis. *Mini Rev Med Chem* **6**:867-874.

Winzen R, Kracht M, Ritter B, Wilhelm A, Chen CY, Shyu AB, Muller M, Gaestel M, Resch K and Holtmann H (1999) The p38 MAP kinase pathway signals for cytokine-induced mRNA stabilization via MAP kinase-activated protein kinase 2 and an AU-rich region-targeted mechanism. *Embo J* **18**:4969-4980.

Zhang J, Shen B and Lin A (2007) Novel strategies for inhibition of the p38 MAPK pathway. *Trends Pharmacol Sci* **28**:286-295.

Zhu T and Lobie PE (2000) Janus kinase 2-dependent activation of p38 mitogen-activated protein kinase by growth hormone. Resultant transcriptional activation of ATF-2 and CHOP, cytoskeletal re-organization and mitogenesis. *J Biol Chem* **275**:2103-2114.

JPET Fast Forward. Published on September 5, 2008 as DOI: 10.1124/jpet.108.139006
This article has not been copyedited and formatted. The final version may differ from this version.

Legends for Figures:

Figure 1. Kinase profiling of pamapimod.

A. Pamapimod was profiled against 350 kinases at Ambit Biosciences (San Diego, CA) as described in Methods. Circle size is proportional to percent inhibition at the test concentration (10 uM). Largest circle corresponds to 99% inhibition; medium circle corresponds to 90 – 99% inhibition; smallest circles, 50 – 90% inhibition, are discounted because this typically translates to a Kd of greater than 1 uM. The kinase dendrogram was adapted (Manning et al., 2002) and is reproduced with permission from Science (http://www.sciencemag.org) and Cell Signaling Technologies (http://www.cellsignal.com). Individual kinase names can be visualized by magnification in PDF format. B. Structure of pamapimod.

Figure 2. Cellular selectivity of pamapimod for p38 vs Jnk in chondrosarcoma cells.

SW-1353 chondrocytes were stimulated with TNF and analyzed by western blot as described in Methods. JNK activity was measured by phosphorylation of c-Jun and p38 activity was measured by phosphorylation of HSP-27. Green (top panel) indicates phospho-specific antibodies and red (middle panel) indicates total protein. The third panel shows an overlay of two colors to represent relative contribution of phosphorylated and total protein. Pamapimod had no effect on Jnk activity but inhibited p38 with an IC50 of 0.063 uM.

Figure 3. Pamapimod inhibits clinical disease scores in murine collagen-induced arthritis.

Mice were immunized on Day 0 with type II collagen and given an IP injection of LPS four weeks later to accelerate and synchronize disease onset. Following detection of disease as assessed by clinical score, mice were treated for 10 days with pamapimod or dexamethasone (DEX). Pamapimod inhibited disease scores in a dose dependent manner. Both 100 and 150

mg/kg doses produced a statistically significant suppression of disease (* $p < 0.05$; ** $p < 0.01$). The presented data are from a single study representative of three independent experiments.

Figure 4. Bone protection by pamapimod in murine collagen-induced arthritis.

Micro-CT analysis was used to assess the effects of pamapimod on bone density in the murine collagen-induced arthritis model. A. Combined phalanges scores on day 15 post-LPS boost of animals that received 3 – 150 mg/kg of pamapimod. Dose dependent restoration in bone density were observed, reaching significant difference from the vehicle-treated controls at 90 and 150 mg/kg (* $p < 0.05$). Dose of 0 mg/kg represents vehicle control and N represents naive control. B. Representative micro CT images of paws from controls and 150 mg/kg dosed animals. C. Total histology scores corresponding to doses in panel A. Scoring was performed for cartilage degeneration, periosteal new bone, bone resorption, soft tissue proliferation and inflammation, and joint space pannus and exudates for all animals in a single collagen-induced arthritis study. Total histology scores were then calculated. Statistical analysis was by Wilcoxon rank-sum exact tests. Dose dependent response is again evident with significant changes from control achieved at the two highest doses.

Figure 5. Pamapimod inhibits spontaneous TNFα production in RA synovial explants.

A. Dissociated human RA synovial membrane mixed cell populations were incubated with pamapimod for 2 days, then levels of TNFα in the culture supernatant were determined by ELISA and the percent inhibition calculated**.** Data are triplicates pooled from 8 donors. Spontaneous TNFα levels range from 170-2630 pg/ml (n=8, mean = 947 pg/ml SD = 851). B. Identical culture system using SB203580 instead of pamapimod. Data are triplicates from 3 donors.

Fig 6. Efficacy of R9111 in MRL/lpr mouse lupus. Spontaneously lupus-prone MRL/lpr mice were treated by minipump with the p38 inhibitor R9111 or dexamethasone (Dex) at the doses indicated for 2 weeks duration beginning at 12-14 weeks of age. A) Renal perivasculitis scores reflected the sum of perivascular scores as assessed in the papillary, arcuate and peri-renal regions on histopathology. For statistical analysis, data were transformed to the ranks of the data and one-way ANOVA was applied (**$p < 0.01$). B) Proteinuria was assessed via determination of protein/creatinine ratio in urine. Log transformation was applied to assure normality and one-way ANOVA was applied (**$p < 0.01$). C) Whole lung of animals (3 animals for each treatment group) were assessed by western blot for phospho-Hsp25, phospho-p38, total Hsp25, and total p38.

JPET Fast Forward. Published on September 5, 2008 as DOI: 10.1124/jpet.108.139006
This article has not been copyedited and formatted. The final version may differ from this version.

Table 1. Selectivity of pamapimod determined by Ambit profiling.

Kinase	Kd (nM)*
P38α	1.3
P38β	120
Jnk1	190
Jnk2	16
Jnk3	19
Caseine Kinase 1ε	260
NLK	170
RSK2**	300
RSK4**	150

* Kds were determined for all kinases that demonstrated greater than 85% inhibition.
** Kinase domain 2 (C terminal kinase)

JPET Fast Forward. Published on September 5, 2008 as DOI: 10.1124/jpet.108.139006
This article has not been copyedited and formatted. The final version may differ from this version.

Table 2. p38 isoform selectivity of pamapimod. Pre-activated recombinant p38 isoforms were assayed for activity by 33-P incorporation into myelin basic protein substrate in the presence of varying concentrations of pamapimod as described.

	IC50 (uM)*	IC75 (uM)*
p38α	0.014 ± 0.002	0.098 ± 0.014
p38β	0.48 ± 0.04	3.32 ± 2.0
p38γ	>100	>100
p38δ	>100	>100

*IC50 and IC75 values are expressed ± SEM.

JPET Fast Forward. Published on September 5, 2008 as DOI: 10.1124/jpet.108.139006
This article has not been copyedited and formatted. The final version may differ from this version.

Table 3. In vitro efficacy of pamapimod on LPS-induced cytokine production by THP-1 cells and human whole blood (HWB).

Efficacious Concentration	In Vitro		
	THP-1	HWB	
	TNFα	TNFα	IL-1β
IC50 (uM)*	0.025 ± 0.01	0.40 ± 0.16	0.10 ± 0.03
IC75 (uM)*	0.12 ± 0.05	2.90 ± 1.23	0.43 ± 0.10

*IC50 and IC75 values are expressed ± SEM.

JPET Fast Forward. Published on September 5, 2008 as DOI: 10.1124/jpet.108.139006
This article has not been copyedited and formatted. The final version may differ from this version.

Table 4. Effects of pamapimod on acute inflammation in vivo using LPS- and TNF-stimulated cytokine production in rodents and a rat model of hyperalgesia. For the yeast-induced hyperalgesia experiments, pamapimod was tested at 10 – 100 mg/kg. Doses of 30 and 100 mg/kg did not differ significantly from the positive control indomethacin (i.e. produced maximum inhibitory response).

Assay	LPS-induced TNFα (rat)	LPS-induced IL-6 (rat)	LPS-induced TNFα (mouse)	LPS-induced IL-6 (mouse)	TNF-induced IL-6 (rat)	Yeast-induced hyperalgesia (rat)
ED50 (mg/kg)*	0.3 ± 0.07	0.1 ± 0.03	1.0 ± 0.07	0.5 ± 0.21	1.1 ± 0.33	20.4 ± 4.8
EC50 (uM)*	0.12 ± 0.02	0.05 ± 0.03	0.17 ± 0.02	0.10 ± 0.04	0.27 ± 0.17	4.3 ± 0.67

*Data represent results from three independent mouse experiments or two independent rat experiments. Means are presented ± ASE (asymptotic standard error).

JPET Fast Forward. Published on September 5, 2008 as DOI: 10.1124/jpet.108.139006
This article has not been copyedited and formatted. The final version may differ from this version.

Figure 1.

A.

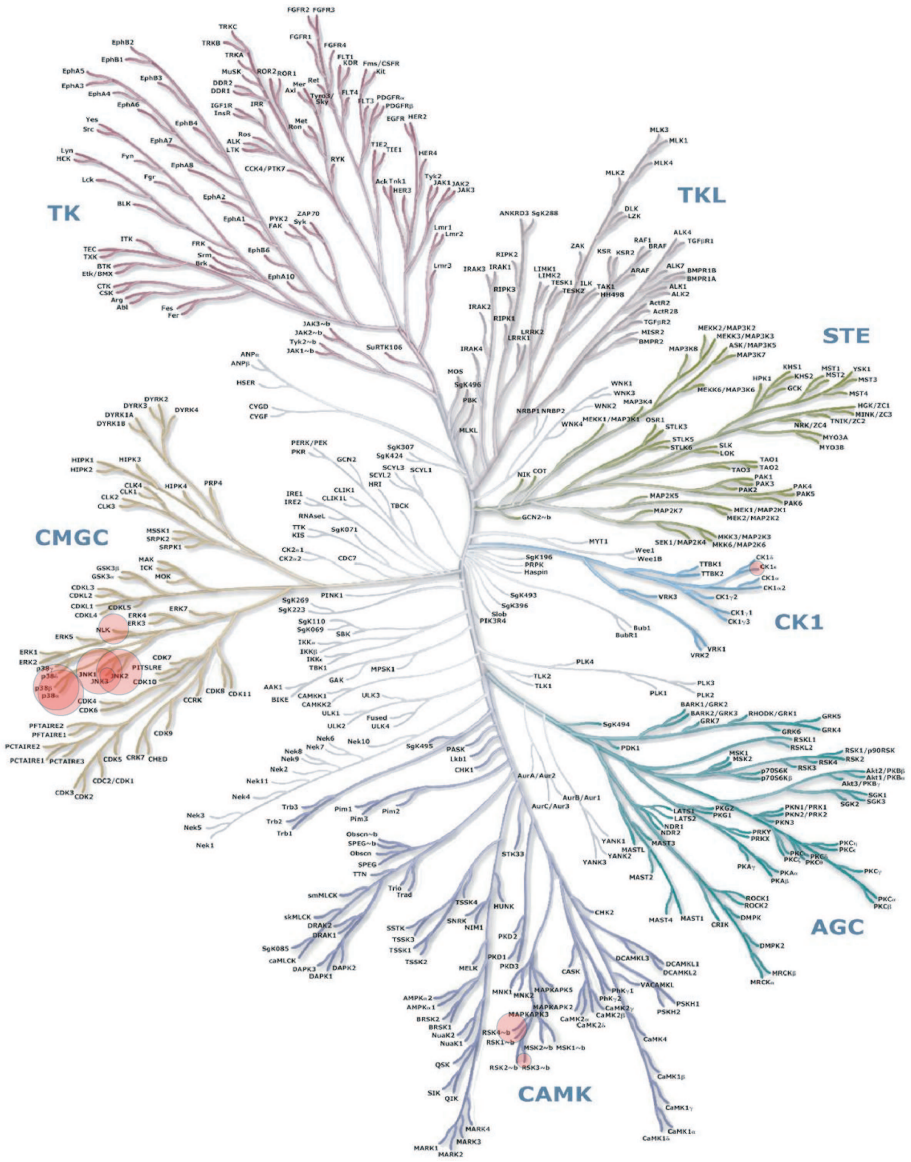

B.

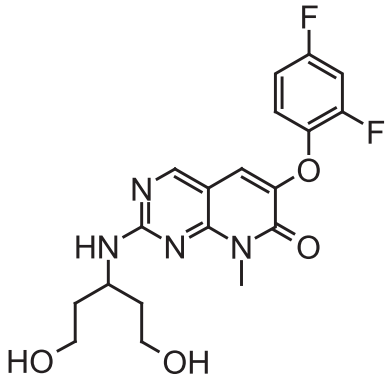

JPET Fast Forward. Published on September 5, 2008 as DOI: 10.1124/jpet.108.139006
This article has not been copyedited and formatted. The final version may differ from this version.

Figure 2.

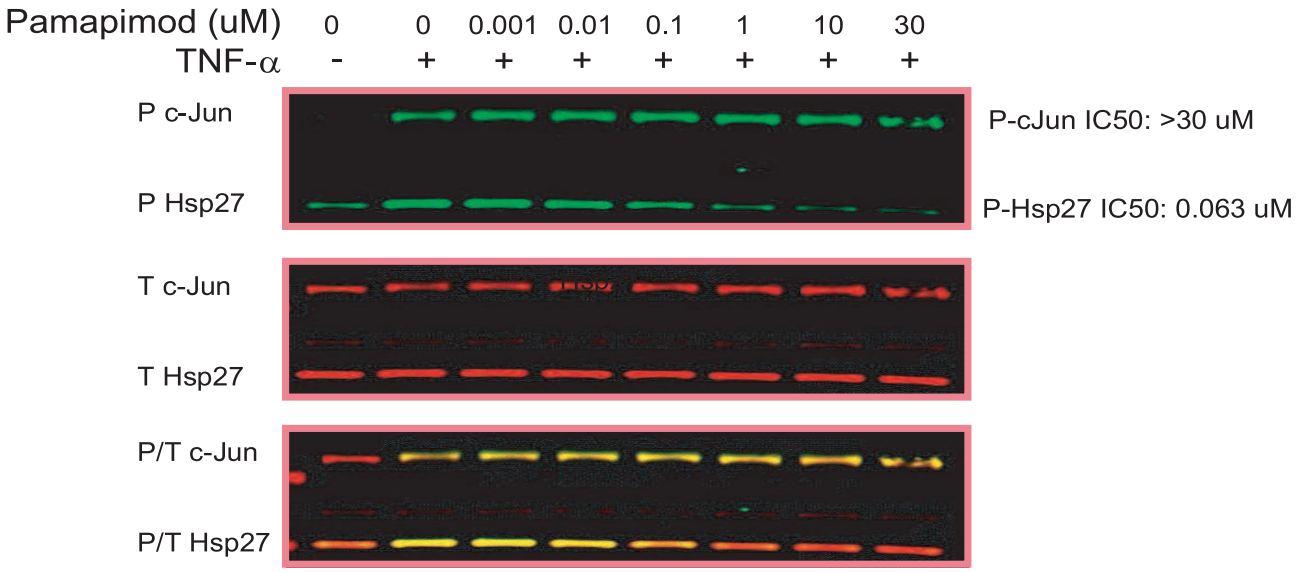

JPET Fast Forward. Published on September 5, 2008 as DOI: 10.1124/jpet.108.139006
This article has not been copyedited and formatted. The final version may differ from this version.

Figure 3.

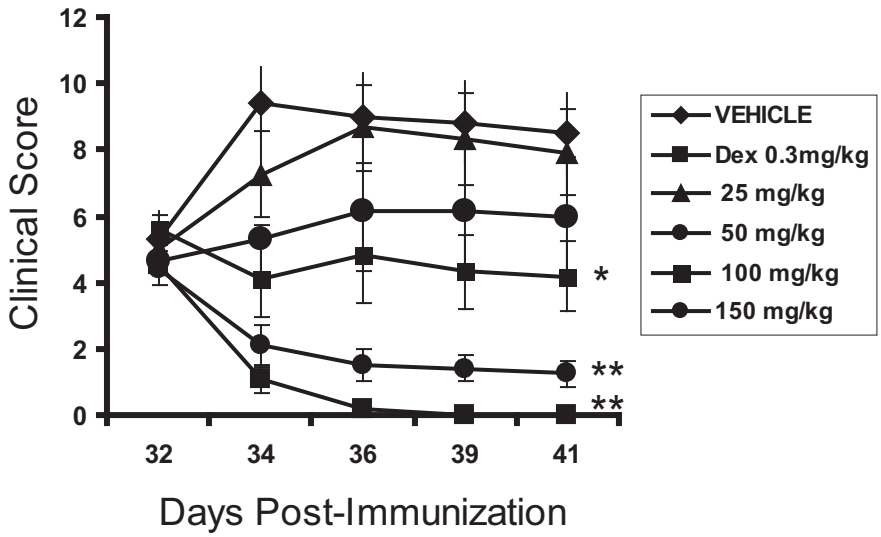

JPET Fast Forward. Published on September 5, 2008 as DOI: 10.1124/jpet.108.139006
This article has not been copyedited and formatted. The final version may differ from this version.

Figure 4.

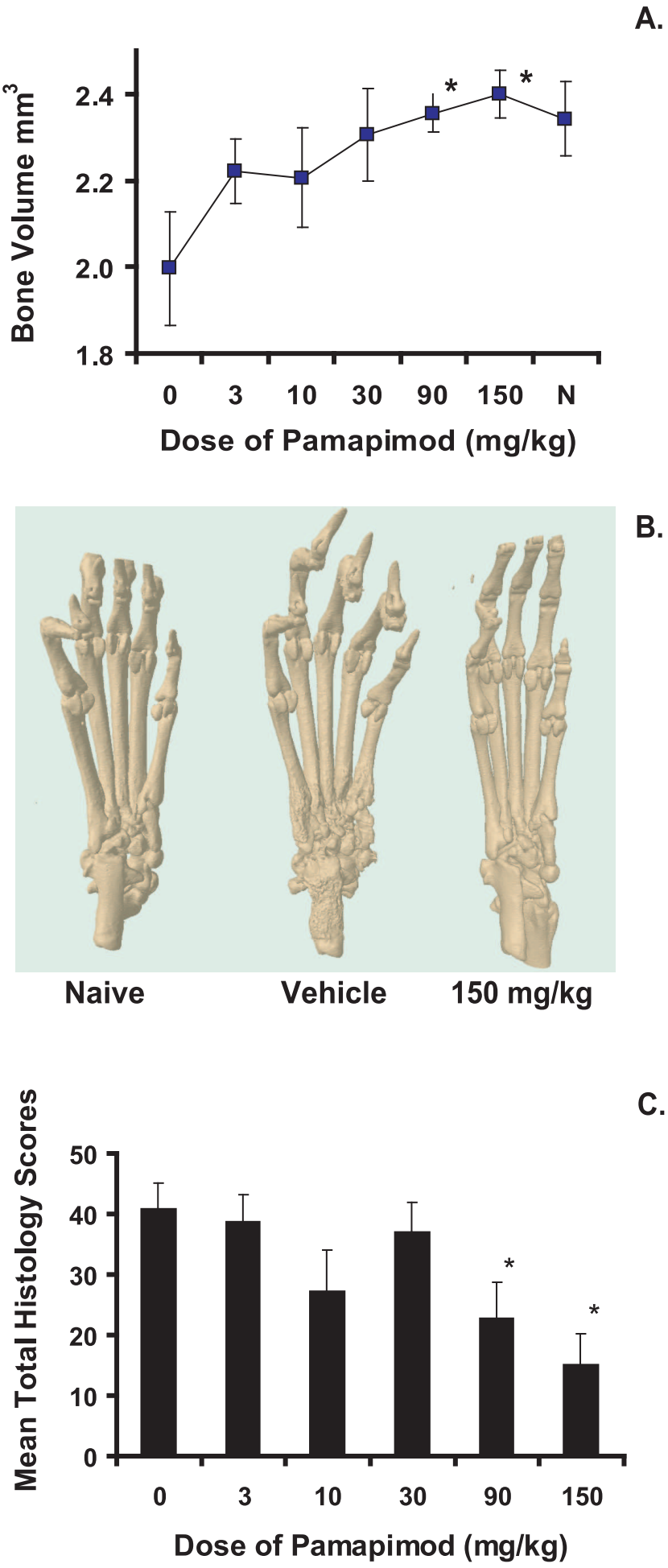

JPET Fast Forward. Published on September 5, 2008 as DOI: 10.1124/jpet.108.139006
This article has not been copyedited and formatted. The final version may differ from this version.

Figure 5.

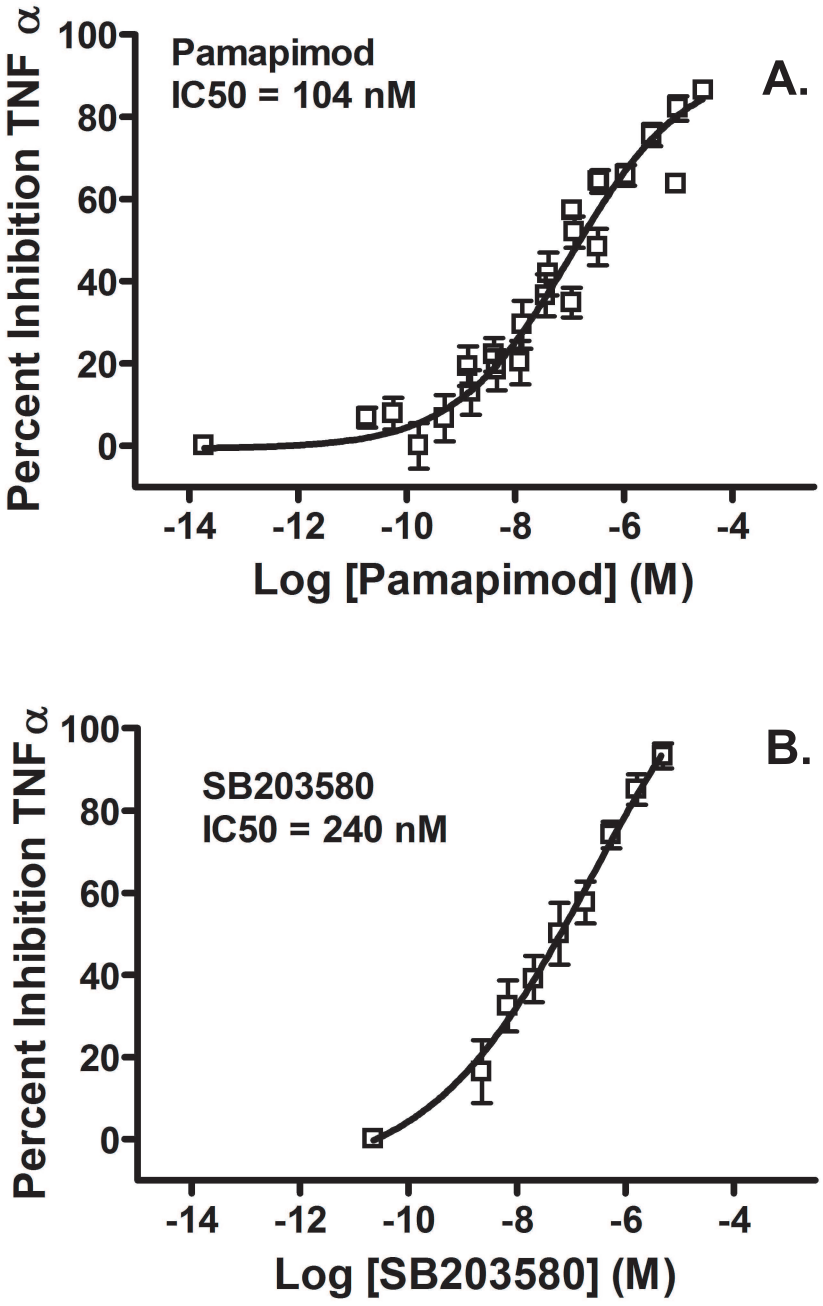

Figure 6.

JPET Fast Forward. Published on September 5, 2008 as DOI: 10.1124/jpet.108.139006